Design and testing of stability improvement of nine multi-level H-inverter for distribution system

R. Arulmurugan
Department of EE, Sanjivani College of Engineering, Kopargaon, Maharashtra, India

Article Info	ABSTRACT
	In this article, a solitary phase nine-level series connected H-Bridge powered by photovoltaic MPPT based SHAPF in view of basic controller is proposed. SRF is utilized for reference input current extraction and to create pulses for the SHAPF. The principle point of the cascaded bridge is to dispense harmonics, enhance power factor and reactive energy compensation of the single-phase distribution framework. The suggested control calculation has two parts, changing the load current into stationary reference outline directions and estimation of peak amplitude of load currents. Consequently, a basic and dependable controller effortlessly of execution was created. The calculation for single-phase SHAF is intending to perform with exact tracking performance under step changes in load currents and to give great dynamic compensation. In this article, synchronous reference theory PLL with Inverse-Park change is adopted for producing quadrature part of current. The execution of the control calculation is tried and assessed utilizing MATLAB/Simulink tool.

Corresponding Author:

R. Arulmurugan,
Professor at Department of EE, Sanjivani College of Engineering,
Kopargaon, Maharashtra, India.
Email: arul.lect@gmail.com

1.   INTRODUCTION

In last years, harmonics is the most essential issue as far as power quality because of wide-spread of energy conversion or power electronic gadgets in business, mechanical and residential loads. In dissemination frameworks, the usage of non-linear loads, for example, PCs, variable/flexible speed drives, light emitting device frameworks and conservative fluorescent lamps and so onward are utilizing generally and inclined to harmonics [1]. These harmonics are causing serious issues, for example, control power losses in equipment's, breaking down or malfunctioning of gadgets, harming of delicate loads and drive engine disappointments. Subsequently, it is a genuine concern in distribution frameworks for both purchasers and providers to dispose of harmonics and meet the necessities of IEC 61000-3-2 or IEEE 519-1992 [2].

The harmonics created by the loads are making grid voltages be mutilated. Traditionally, detached filters are utilized for harmonic alleviation and reactive power compensation. In any case, these experience the ill effects of weaknesses like, massiveness, cost, resonance and fixed remuneration [3]. In such a way, a dynamic arrangement is favored that fits the compensation is a shunt active filter. The role of APF is to compensate reactive power and harmonic currents with enhanced power factor delivered by the load. The controller needs to path the progression changes in the load precisely and to choose reference current appropriately for better compensation.

Keeping reliability and accuracy in view, numerous methods are explained in surveys for quadrature signal production. ZCD technique [4] is straightforward at the same time, sensitive to variations of grid. In general the utilized technique is SRFR and SOGI based hypothesis [4-6]. It is less precise to unequal and brings down harmonic components. Be that as it may, SRF hypothesis with reverse stop change based

calculation is discovered palatable under contorted conditions with low computational burden. In any case, application and usage of this control process for a five level cascaded H-connect dynamic power filters has not increased much consideration in the literature.

MLI have increased much consideration in virtue of its gigantic preferences over traditional voltage source inverters. The traditional two-level inverter is likewise fit for taking care of harmonic reduction, power factor change and reactive power under different load changes. Yet, because of progression of electronic gadgets and controllers, MLIs have demonstrated their capacity to compensate issues of power quality with straightforwardness, ease, dependability and high-quality output. There are numerous methods suggested in the literature [7-9], Flying capacitor based inverter, neutral point clamped inverter and cascaded H-connected type MLI is discovered reasonable for SHAPF application effortlessly of control.

In this article, cascade H- bridge sort of MLI is utilized to lessen the ranking of the gadgets utilized and disposal of harmonics with an expansion in levels of the converter. This technique likewise lessens the exchanging misfortunes and declines the ratings of the direct current interface capacitors utilized. The control calculation is discovered effective in linear/ non-linear and increment in load circumstances. With a specific end goal to every one of these topologies, different PWM strategies were likewise suggested in the surveys which incorporates specific harmonic disposal based PWM, Carrier based PWM, Multilevel space vector based PWM and so on [10-22]. The fundamental favorable position of this CHB inverter is expanding of switching levels by increasing the number of H-connected in the circuit. This paper utilizes a basic SRF based control in with reverse park alteration to generate quadrature signal for reactive power compensation and harmonic minimization.

A cascade H-bridge based SHAF is proposed in this article, Non-linear load cases under steady state and dynamic conditions are completed utilizing Simulink, simpower frameworks block set and its execution discovered palatable.

2.   DESIGNED CONFIGURATION AND CONTROLLER

The Cascade H converter based SHAPF appeared in Figure 1. Every H-connect comprises of a two-leg VSC comprising of 4 IGBT switches. There are two H-connect VSC's are utilized for producing five level yield over the inverter as appeared in Figure 2. SHAF is associated in middle of source and load in parallel through an interfacing inductor L_f at the PCC. The recommended controller for SHAF is equipped of keeping up the THD within the limits by removing the harmonics in the input or grid current. Reactive power, Power factor rectification, and harmonic compensation is likewise done even under changing non-linear and linear load situations to examination the execution of the controller. The SHAF can be worked with required dynamic and responsive power infusion by modifying the greatness and phase of the system. The ratings of the designed framework are listed in reference section. The rating of the SHAF ought to be 15% more than the Load rating for more secure and monetary operation.
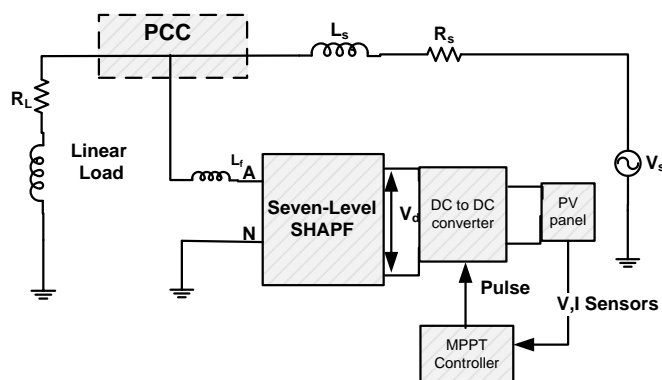

Figure1. Line chart of the proposed system

2.1. SRF-PPL

At present, the essential PLL topology generally utilized in all the area of research is SRF based PLL as appeared in Figure 2. V represents as input voltage signal and is considered as V_α and its orthogonal part that is moved by 90^0 is V_β. These two parts (V_α and V_β) are in constant reference frame and these are changed over to synchronous turning reference frame (d,q) by utilizing Park's transformation [6].

$$T = \begin{bmatrix} \cos \hat{\theta} & \sin \hat{\theta} \\ -\sin \hat{\theta} & \cos \hat{\theta} \end{bmatrix} \tag{1}$$

The d-q parts in its reference outline are controlled by a precise position with a feedback signal related with it. The grid voltage amplitude is thoroughly relating with the d-segment and corresponds with all its d–segment and furthermore making q-part to zero. The transformation yield is gone through a circle channel (LF) for taking out any high frequency noises within it and afterward included with the nominal frequency and afterward provided to a VCO to create central stage point θ. So as to get a correct amplitudes with an adjusted arrangement of quadrature yields and in-phase, the frequency produced by the phase locked loop ought to be equivalent to the input fundamental frequency ($W_{ff}=2\pi*50$). Proportional Integral controller is the essential loop filter utilized as a part of all these PLL topologies.
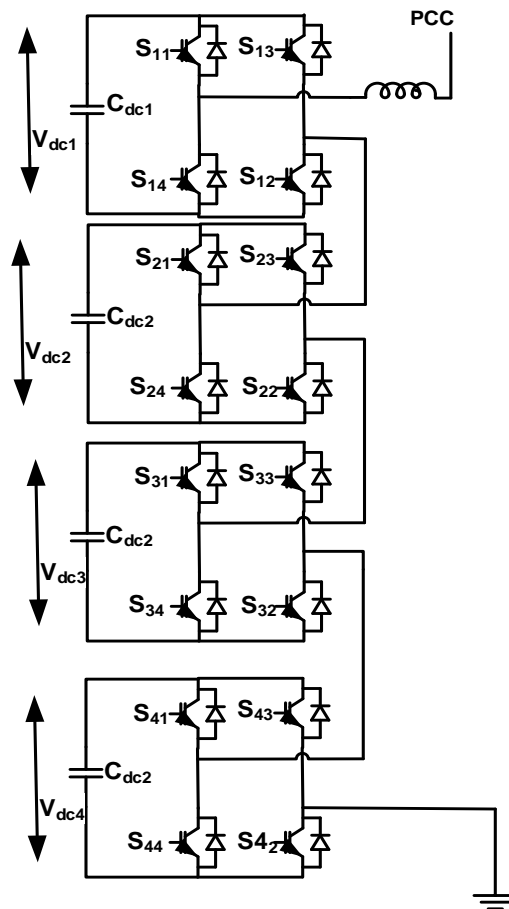

Figure 2. Designed H-connected cascaded multilevel inverter

2.2. Inverse park transformation
Figure 3. demonstrates the structure of inverse park transformation. Park transformation is done (i.e, αβ0/dq0s) and these yields are utilized for opposite park alteration as appeared in Figure 3. The elements of the phase indicator predominantly relies the low pass filter that is utilized after the transformation to filter out any noises or harmonics that are available in V_d and V_q.
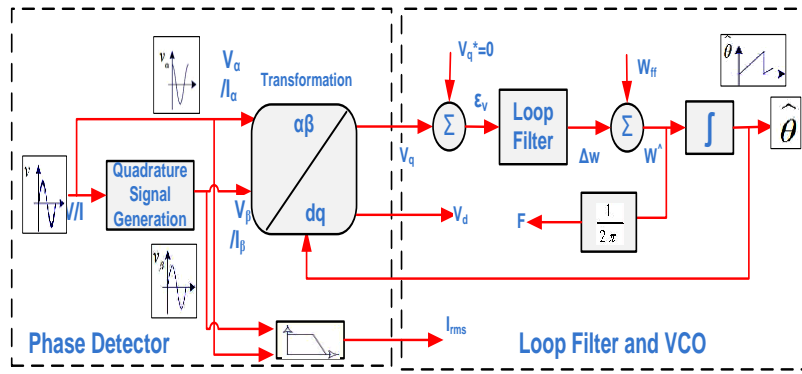
Figure 3. Control diagram of SRF–PLL

2.3. Reference current generation

The peak amplitude of active segment of current is computed as appeared in Figure 4. The load current is detected and provided to inverse park transformation to create quadrature signals ($I_{L\alpha}$ and $I_{L\beta}$) and afterward changed back to I_d and provided to a low-pass filter. The yield is then included with the output created by the DC voltage control circle to deliver reference dynamic part of current ($I_{LP}+I_{CD}$). The deliberate voltage (V_{dc}) over the two DC capacitors are summed and contrasted and the direct current bus reference voltage ($V_{dc}{}^{*}$). The error of the signal at n^{th} examining moment is given by:

$$V_d(n)=V^*{}_{dc}(n)-V_{dc}(n) \tag{2}$$

The voltage error $V_d(n)$ is then provided to Proportional-Integral controller to direct the DC bus voltage of SHAPF. At n^{th} examining moment, the yield of the PI controller is as:

$$I_{cd}(n)=I_{cd}(n-1)+k_p\{V_{dcer}(n)-V_{dcer}(n-1)\}+k_iV_{dcer}(n) \tag{3}$$

Where, K_p and K_i are proportional gain and integral gains of the PI controller. $V_{dcer}(n)$ and $V_{dcer}(n-1)$ are the direct current bus voltage errors in n^{th} and $(n-1)^{th}$ moment and $I_{cd}(n)$ and $I_{cd}(n-1)$ are the amplitudes of dynamic segment of currents at the basic reference current in n^{th} and $(n-1)^{th}$ moment.

The magnitude current (I_{LP}) and the yield of the proportional integral controller (I_{cd}) are summed up to altered I_α (source current reference) from dq0 part and afterward contrasted with the genuine source or grid current to create error magnitude of current and after that provided to a pulse width modulation controller to produce pulses to MLI.
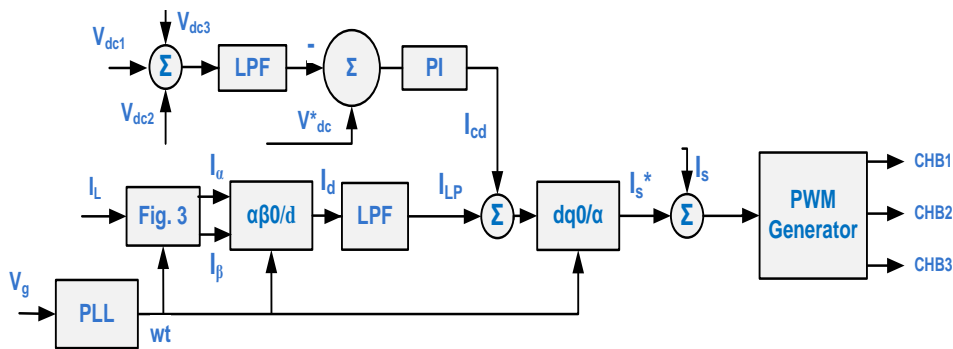

Figure 4. Control modes of RSC generation

3. MODELLING OF PHOTOVOLTAIC PANEL

The modeling of photovoltaic array panel can be applied from the mathematical classical in Equation (4), which is consequent from the cell equivalent circuit where every cells are identical [22].

$$I_P = N_p.I_{PH} - N_P.I_O \left[e \left(\frac{q(V_{PV} + R_S I_{PV})}{AKTN_S} \right) - 1 \right] - N_P \frac{(V_{PV} + R_S.I_{PV})}{R_{HS}.N_S}$$ (4)

Where I_{pv} is the photovoltaic panel current, V_{pv} is the photovoltaic output voltage, R_S is the cell series resistance, q is the electron charge in 1.6×10^{-19} C, R_{sh} is the cell parallel resistance, I_{ph} is the light produced current, k represents the Boltzmann constant generally 1.38×10^{-23} J/K, A is dimensionless factor, I_O is the reverse saturation, T denoted temperature in K, N_S and N_P symbolize no. of cells jointed in series and parallel respectively. Generally, every photovoltaic cell is basically formed as a P-N junction. It converts sunlight energy into electrical power with no environmental issues. The Equivalent model of photovoltaic system is shown Figure5.

When recommending a MPPT, the most important job is to select and analysis an effective converter, which is hypothetical to function as the major role of the maximum power extraction [11]. The direct current to direct current boost converter offers a positive sign controlled output voltage with respect to the input source voltage is exposed. The step up converter is utilized to increases the secondary voltage of converter. This converter desires one inductor, switch and diode [12]. The output voltage of step up converter is always greater than the primary voltage magnitude. Therefore, this boost converter generally connects high load or battery voltages. Normally the step up converter cannot reproduce impedances that are larger than impedance of load value. So the step up converter does not attain values nearby a PV modules open circuit voltage. That means R_{load} is always less than equal to R_{mpp}. The MPPT will be traced as if it is limited to within the operating region.
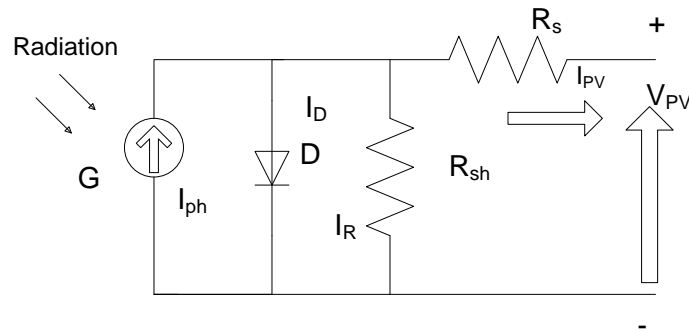

Figure 5. Solar cell equivalent model circuit

For improving the efficacy of the output power of the photovoltaic panel and the inverter a MPPT with control algorithm are introduced. The control algorithm is necessary because photovoltaic panel characteristics have a non-linear current vs. voltage with a unique point where the power produced is higher. This point reflects the temperature and irradiation of the situation. These conditions are change throughout day and season of the year. So it is essential to track the MPP accurately under all possible situations using MPPT approach. In this paper P&O approach used to track the possible power point. The P&O method have function as a perturbation in the operating voltage of the direct current link between the PV panels boost converters. The perturbing the duty cycle of the step up converter infers adjusting the voltage of the direct current link of the power converter. The algorithm function on the sign of the previous perturbation and the sign of the previous increment in the power are utilized to select what the subsequent perturbation must be.

The photovoltaic are demonstrated as nonlinear sources voltage. The sources are associated with direct current to direct current converters which are joined at the direct current side of a inverter (DC/AC). The DC/DC associated with the PV array operates as a MPPT controller. Numerous MPPT calculations have been offered in the script, for example, Incremental Conductance (INC), Constant Voltage (CV), Perturbation and Observation (P&O). The P&O technique has been broadly utilized in view of its basic and simple feedback structure and less measured parameters [7]. The P&O calculation with control input control [8–10] is appeared in Figure 6. As PV voltage and current are resolved, the power is computed. At the MPP, the derivative (dP/dV) is equivalent to zero. The greatest power point can be accomplished by changing the reference voltage by the measure of ΔVref.
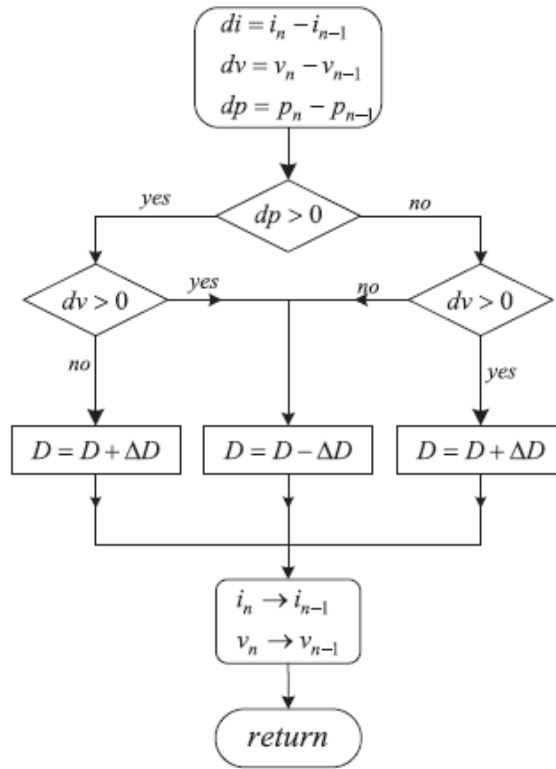
$$di = i_n - i_{n-1}$$
$$dv = v_n - v_{n-1}$$
$$dp = p_n - p_{n-1}$$

yes $dp > 0$ no

$dv > 0$ yes   no $dv > 0$

no   yes

$$D = D + \Delta D$$ $$D = D - \Delta D$$ $$D = D + \Delta D$$

$$i_n \rightarrow i_{n-1}$$
$$v_n \rightarrow v_{n-1}$$

return

Figure 6. P&O MPPT controlling algorithm

4. SIMULATION TEST AND RESULTS

In this segment, the designed control calculation is assessed and tried utilizing MATLAB/Simulink on a solitary-phase distribution framework loaded with non-linear and linear loads. Settled time step of 20µs with ode3 (Bogacki-Shampine) solver is decided for recreation [23]. Scarcely any experiments are performed for assessments of SHAPF are: The execution of the controller when a nonlinear and linear load is connected is appeared in Figure 7. and Figure 8. when time period t=0.4secs to 0.5secs. All these experiments are executed under sinusoidal grid conditions [24, 25]. The execution under powerful conditions is discovered attractive. The direct current bus voltage control, harmonic compensation and reactive power with power factor change demonstrate the viability of the controller [26]. THD (%) of cases specified above are exhibited in Table 1 demonstrate the viability of the controller.
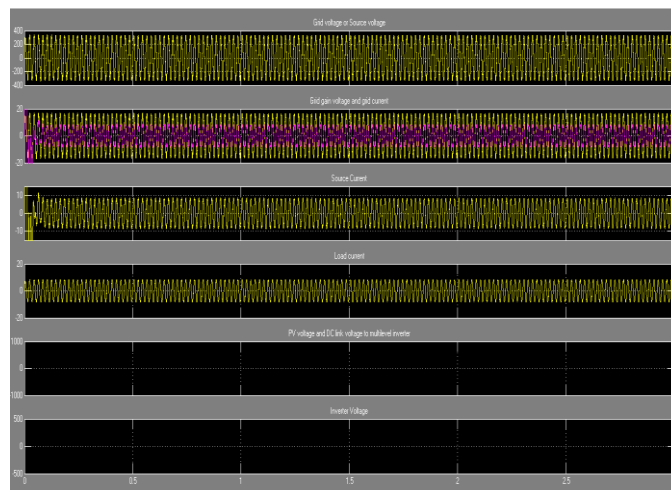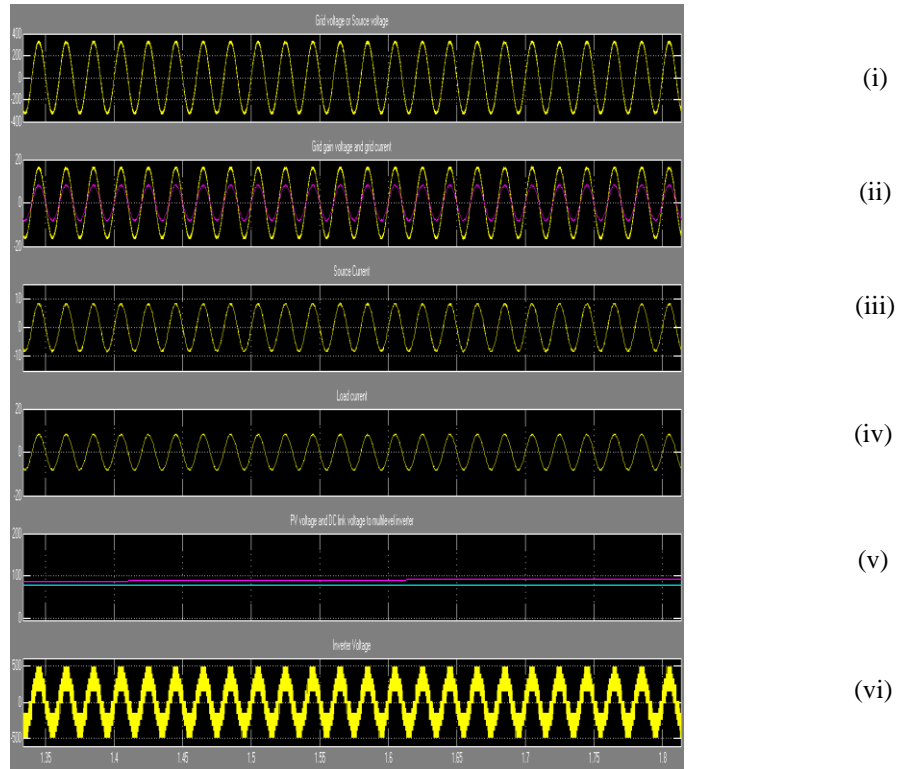

Figure 7(a). Compressed view of the linear system

Figure 7(b). Close view of the linear system;
(i) Source voltage in volts, (ii) Scaled source voltage and source current (iii) Source current (iv) Load current
(v) Injected current (v) DC link voltage in volts of Vdc1 to Vdc4 (vi) Inverter nine level voltage

Figure 7. Performance of nine level cascaded H-connected inverter with linear load

Table 1. THD (%) of test cases

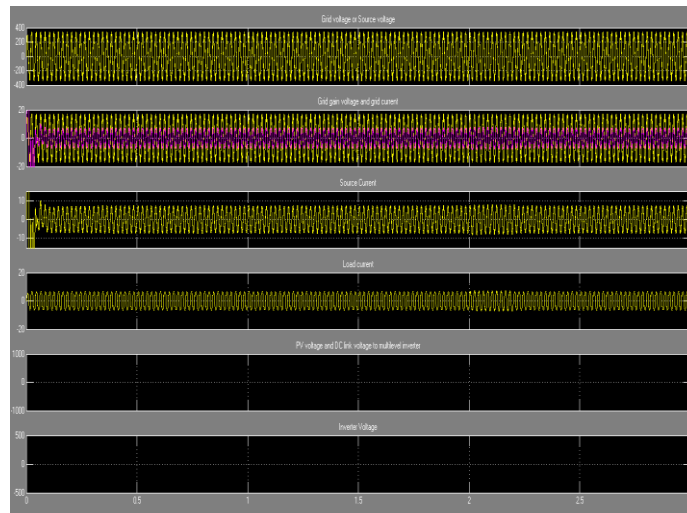| No of switching converter	THD level	
Type of load	Non-Linear load	linear load
Fundamental (50Hz)	333.7	325.4
Proposed Nine level PV	17.95%	42.06%

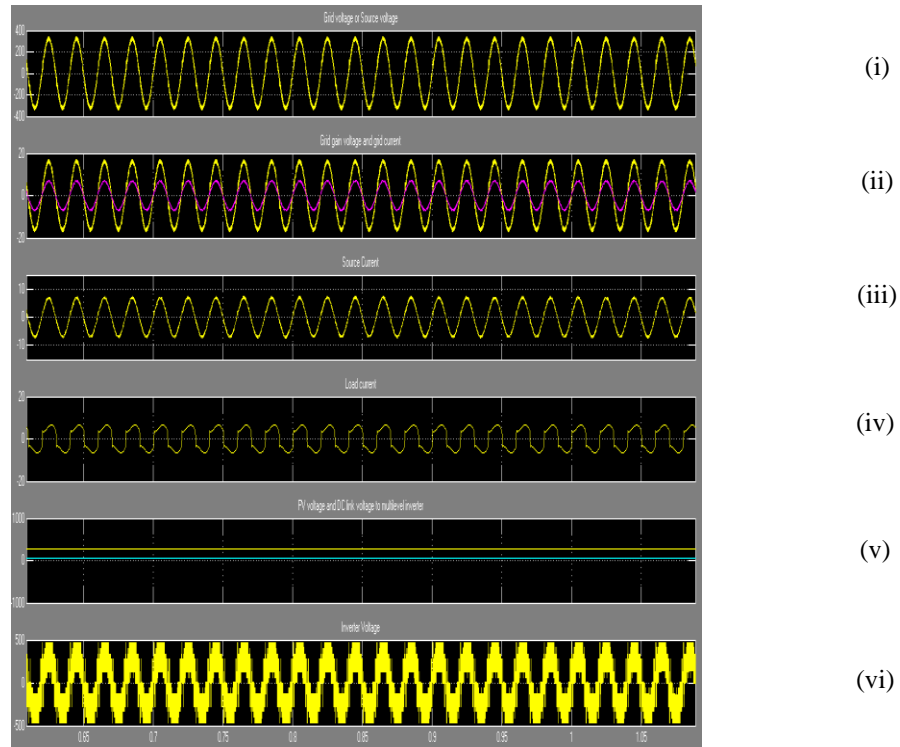Figure 8(a). Compressed view of the non-linear system

Figure 8(b). Close view of the non-linear system;
(i) Source voltage in volts, (ii) Scaled source voltage and source current (iii) Source current (iv) Load current
(v) Injected current (v) DC link voltage in volts of Vdc1 to Vdc4 (vi) Inverter nine level voltage

Figure 8. Performance of nine level cascaded H-connected inverter with non-linear load

Figure 9. proves the nine-level output of multilevel inverter. Followed by, Figure 9. shows the pulse chart of single bridge system. Each bridge system used the four switches, The Figure 10. shows one bridge circuit of four switching pulses. Followed by THD levels of non-linear and linear waveforms were displaced in Figure 11. The non-linear and linear of nine-level THD values were associated with non PV nine-level inverter as exposed in Table 1. Table 1. proves that the nine-level inverter reduced the harmonics level more than 15% than nine-level systems.
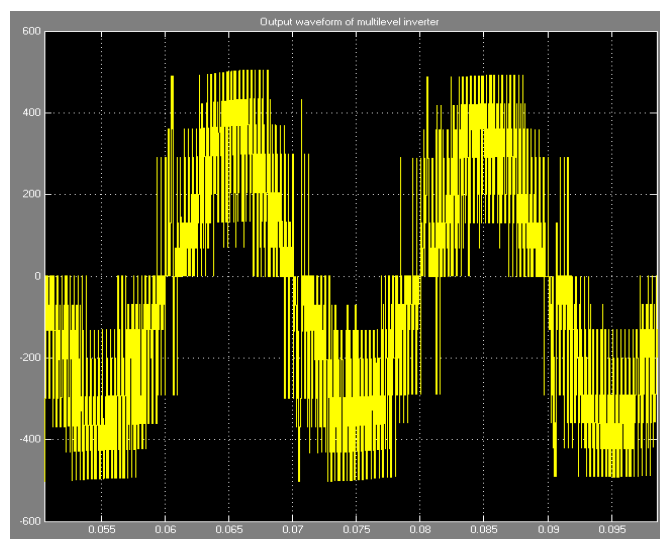

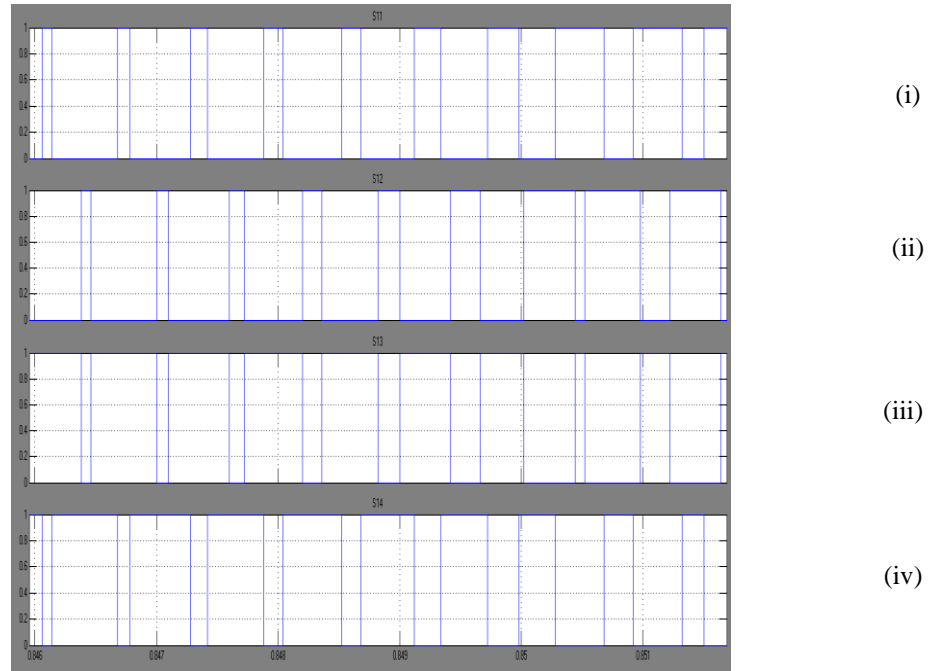Figure 9. Nine-level cascaded H-connected bridge output voltage waveform

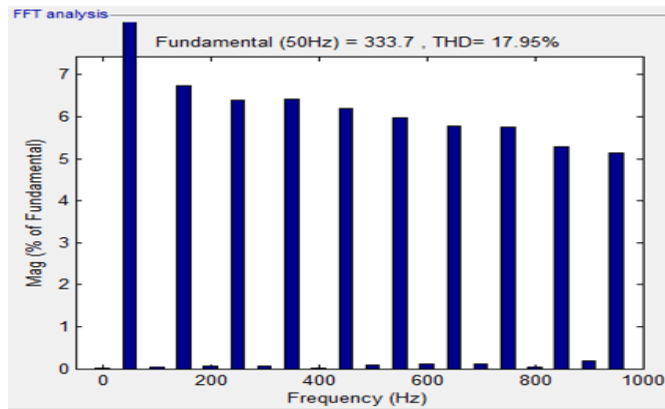Figure10. Pulse output waveforms of single bridge inverter (i) S11 (ii) S12 (iii) S13 (iv) S14
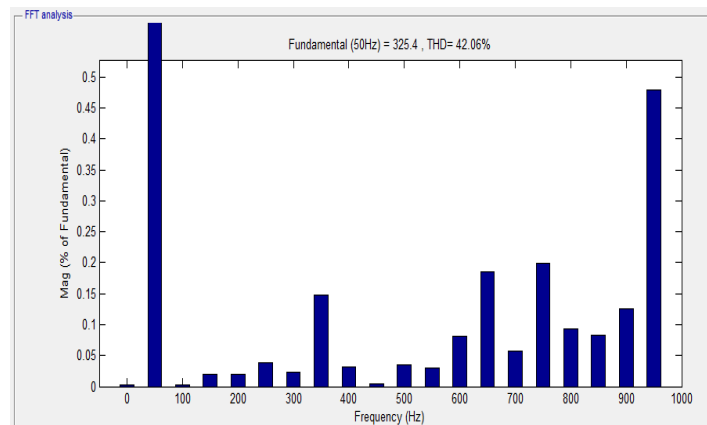

Figure 11 (a). Non-linear system

Figure 11(b). Linear system

Figure 11. THD examination of the designed PV nine-level inverter

5.   CONCLUSION

In this article, a basic and compelling control calculation in view of Synchronous Reference Frame (SRF) hypothesis for single-phase system with photovoltaic MPPT powered cascaded nine-level H-connected dc to ac converter has been analyzed, exhibited utilizing MATLAB/Simulink tool. This hypothesis is embraced to work in sinusoidal grid voltage conditions and Non-Linear load situations. The source or grid current harmonics THD(%) is kept up IEEE 519-1992 breaking points. The control calculation is tremendously encouraging and simple to execute due to its straightforward structure and exactness. The reactive current, harmonic compensation and power factor is effectively done under all relentless-state and dynamic situations. The infused current of the shunt active device of power factor was likewise near the reference esteems and demonstrated a smooth and dependable profile.

APPENDIX

Grid Voltage & Frequency	Single-Phase, 230V, 50Hz
Source-side Impedance	Rs=0.1 Ω, Ls =2.5mH
Non-linear: Single-phase diode bridge rectifier	R=40Ω, L= 250mH,
Linear Load	R=40 Ω, L=250mH
PWM Switching frequency	2kHz
Reference voltage of DC bus	400V
Interfacing inductor	L_f=1.5mH
Gains of PI controller for DC bus	K_p =0.32, K_i=6

REFERENCES

[1]   IEEE Recommended Practices and Requirements for Harmonic Control in Electrical Power Systems., *IEEE Std*. 519, 1992.
[2]   Electromagnetic Compatibility (EMC)—Part 3-2: Limits—Limits for Harmonic Current Emissions (Equipment Input Current=16 A per Phase), *IEC 61000-3-2*, 2005.
[3]   A. Timbus, M. Liserre, R. Teodorescu, and F. Blaabjerg, "Synchronization Methods for Three Phase Distributed Power Generation Systems: an Overview and Evaluation," *IEEE PESC 2005*, pp. 2474-2481, 2005.
[4]   Kaura and V. Blasco, "Operation of a Phase Locked Loop System under Distorted Utility Conditions," *IEEE Trans. Ind. Appl.*, Vol. 33, no. 1, pp. 58–63, 1997.
[5]   Yada, Hareesh Kumar, and M. S. R. Murthy, "A New Topology and Control Strategy for Extraction of Reference Current using Single Phase SOGI-PLL for Three-Phase Four-Wire Shunt Active Power Filter", *2014 IEEE International Conference on Power Electronics Drives and Energy Systems (PEDES)*, 2014.
[6]   Yada, Hareesh Kumar, and M. S. R. Murthy. "Phase Locked Loop Techniques for Power Quality Improvement in Polluted Grids", *2016 IEEE International Conference on Power Electronics, Integrated Circuits and Energy Systems (ICPEICES)*, 2016.
[7]   K. H. Law, M. S. A. Dahidah, and N. Marium, "Cascaded Multilevel Inverter based STATCOM with Power Factor Correction Feature," *Proc. IEEE Conf. Sustainable Utilization Develop. Eng. Technol.*, pp. 1–7, 2011.
[8]   F. Z. Peng and J. S. Lai, "Dynamic Performance and Control of a Static Var Generator using Cascade Multilevel Inverters," *IEEE Trans. Ind. Appl.*, vol. 33, no. 3, pp. 748–755, Jun. 1997.
[9]   Y. Cheng, Q. Chang, L. C. Mariesa, S. Pekarek, and S. Aticitty, "A Comparison of Diode-Clamped and Cascaded Multilevel Converters for a STATCOM with Energy Storage," *IEEE Trans. Ind. Electron.*, vol. 53, no. 5, pp. 1512–1521, Oct. 2006.
[10] R. Naderi and A. Rahmati, "Phase-Shifted Carrier PWM Technique for General Cascaded Inverters," *IEEE Trans. Power Electron.*, vol. 23, no. 3, pp. 1257–1269, May 2008.
[11] W. Yao, H. Hu, and Z. Lu, "Comparisons of Space-Vector Modulation and Carrier-Based Modulation of Multilevel Inverter," *IEEE Trans. Power Electron.*, vol. 23, no. 1, pp. 45–51, Jan. 2008.
[12] J. Rodriguez, L. Moran, P. Correa, and C. Silva, "A Vector Control Technique for Medium-Voltage Multilevel Inverters," *IEEE Trans. Ind. Electron.*, vol. 49, no. 4, pp. 882–888, Aug. 2002.
[13] G. Narayanan and V. T. Ranganathan, "Extension of Operation of Space Vector PWM Strategies with Low Switching Frequencies using Different Overmodulation Algorithms," *IEEE Trans. Power Electron.*, vol. 17, no. 5, pp. 788–798, Sep. 2002.
[14] S. Wei, B. Wu, F. Li, and C. Liu, "A General Space Vector PWM Control Algorithm for Multilevel Inverters," *IEEE Appl. Power Electron. Conf. Expo.*, vol. 1, pp. 562–568, Feb. 2003.

[15] K. Gupta and A. M. Khambadkone, "A General Space Vector PWM Algorithm for Multilevel Inverters, Including Operation in over Modulation Range," *IEEE Trans. Power Electron.*, vol. 22, no. 2, pp. 517–526, Mar. 2007.

[16] W. Yao, H. Hu, and Z. Lu, "Comparisons of Space-Vector Modulation and Carrier-Based Modulation of Multilevel Inverter," *IEEE Trans. Power Electron.*, vol. 23, no. 1, pp. 45–51, Jan. 2008.

[17] M. S. A. Dahidah and V. G. Agelidis, "Selective Harmonic Elimination PWM Control for Cascaded Multilevel Voltage Source Converters: A Generalized Formula," *IEEE Trans. Power Electron.*, vol. 23, no. 4, pp. 1620–1630, Jul. 2008.

[18] Ozpineci, L. M. Tolbert, and J. N. Chiasson, "Harmonic Optimization of Multilevel Converters using Genetic Algorithms," *Proc. Power Electron. Spec. Conf.*, pp. 3911–3916, 2004.

[19] G. Agelidis, A. Balouktsis, and M. S. A. Dahidah, "A Five-Level Symmetrically Defined Selective Harmonic Elimination PWM Strategy: Analysis and Experimental Validation," *IEEE Trans. Power Electron.*, vol. 23, no. 1, pp. 19–26, Jan. 2008.

[20] M. S. A. Dahidah and V. G. Agelidis, "Single-Carrier Sinusoidal PWM-Equivalent Selective Harmonic Elimination Five-Level Inverter Control," *Electr. Power Syst. Res.*, vol. 78, no. 11, pp. 1826–1836, Jun. 2008.

[21] M. S. A. Dahidah, G. Konstantinou, and V. G. Agelidis, "SHE-PWM and Optimized DC Voltage Levels for Cascaded Multilevel Inverters Control," *Proc. IEEE Symp. Ind. Electron. Appl.*, pp. 143–148, 2010.

[22] K. H. Law, M. S. A Dahidah, and V. G. Agelidis, "SHE-PWM Cascaded Multilevel Converter with Adjustable DC Sources Control for STATCOM Applications," *Proc. IEEE 7th Int. Power Electron. Motion Control Conf.*, pp. 330–334, 2012.

[23] R. Arulmurugan and T. Venkatesan, 'Research and Experimental Implementation of a CV-FOINC Algorithm Using MPPT for PV Power System," *Journal of Electrical Engineering and Technology*, vol.10, no.1, pp. 30-40, 2015.

[24] R. Arulmurugan and N.Suthanthiravanitha, "Model and Design of Fuzzy-Based Hopfield NN Tracking Controller for Standalone PV Applications," *Elsevier-International Journal of Electric Power Systems Research (IJEPES)*, vol.120, pp.184-193, 2015.

[25] R. Arulmurugan, "Comparative Evaluation of New FLC Controller Based MPPT for a DC to DC Buck-Boost Zeta Converter," *WSEAS Transactions on Power Systems*, vol.11, pp.27-34, 2016.

[26] R. Arulmurugan, *et. al.*, "Tracking of Photovoltaic Power System with New Fuzzy Logic Control strategy," *Journal of Electrical Engineering (JEE)*, Vol. 14, Ed. 4, pp.1-10, 2014.